JOURNAL OF GEOPHYSICAL RESEARCH, VOL. 106, NO. 0, PAGES 1–12, MONTH 2001

Volcano monitoring using the Global Positioning System: Filtering strategies

Kristine M. Larson,[1] Peter Cervelli,[2] Michael Lisowski,[3] Asta Miklius,[4] Paul Segall,[2] and Susan Owen[5]

Abstract. Permanent Global Positioning System (GPS) networks are routinely used for producing improved orbits and monitoring secular tectonic deformation. For these applications, data are transferred to an analysis center each day and routinely processed in 24-hour segments. To use GPS for monitoring volcanic events, which may last only a few hours, real-time or near real-time data processing and subdaily position estimates are valuable. Strategies have been researched for obtaining station coordinates every 15 min using a Kalman filter; these strategies have been tested on data collected by a GPS network on Kilauea Volcano. Data from this network are tracked continuously, recorded every 30 s, and telemetered hourly to the Hawaiian Volcano Observatory. A white noise model is heavily impacted by data outages and poor satellite geometry, but a properly constrained random walk model fits the data well. Using a borehole tiltmeter at Kilauea's summit as ground-truth, solutions using different random walk constraints were compared. This study indicates that signals on the order of 5 mm/h are resolvable using a random walk standard deviation of 0.45 cm/$\sqrt{\text{h}}$. Values lower than this suppress small signals, and values greater than this have significantly higher noise at periods of 1–6 hours.

1. Introduction

Because significant ground deformation results from most forms of volcanic activity, geodesy is an ideal technique for both monitoring and studying active volcanoes. Moreover, ground deformation tends to precede eruptions by hours to months, which makes geodetic monitoring an effective tool for hazard mitigation. The Global Positioning System (GPS) is well-suited for monitoring volcanoes, since once it is installed, a GPS receiver can provide a nearly continuous record of its position as a function of time without a human presence at a potentially dangerous volcanic locale. For these reasons, several networks of continuously recording GPS receivers have been installed at volcanoes around the globe [*Mattiloi et al.*, 1998; *Dixon et al.*, 1997; *Miyazaki and Hatanaka*, 1997].

Most geodetic quality GPS networks installed in the 1990s for crustal deformation studies have been configured so that data from each receiver are downloaded once per day to a central location. The GPS data are then used to estimate 24-hour average positions for each receiver [*Zumberge et al.*, 1997]. Processing begins when precise orbits are available, which is usually within 1–2 days. The obvious disadvantage of using this analysis style is that any deformation that occurs will not be discerned by GPS for ~2 days, depending on the orbit availability. Another limitation of this analysis strategy is that station coordinates are computed only once per day. A much higher solution rate is obviously needed if the dynamics of a rapidly evolving deformation event like a volcanic eruption or dike intrusion are to be understood. A higher solution rate also allows the scientific team operating a GPS network to quickly respond to an event, perhaps allowing the team to install additional instruments. As an example, the January 30, 1997, eruption on Kilauea was preceded by 8 hours of rapid deflation of Kilauea's summit [*Owen et al.*, 2000b]. This information is easily discernable in the GPS estimates but was not available in near real time to the scientists at the nearby U.S. Geological Survey (USGS) Hawaiian Volcano Observatory (HVO).

The goal of this paper and its forthcoming companion paper (P. Cervelli et al., manuscript in preparation, 2001, hereinafter referred to as paper 2) is to describe efforts to upgrade the continuous GPS network at Kilauea Volcano (Figure 1) so that 15-min position estimates are routinely computed in near real time. Since most of the necessary hardware (GPS receivers and telemetry equipment) and infrastructure (computers and internet access) are already in place, more frequent and timely GPS data analysis is an inexpensive method to gain additional information about the volcano. Although GPS is less precise than borehole instruments at short periods [*Stefansson et al.*, 2000], it can still make a valuable contribution to hazards mitigation by providing independent deformation estimates, particularly in remote areas where other geodetic instruments cannot be installed. GPS also has the advantage that it simultaneously measures all three components of position.

2. Geologic Setting of Kilauea Volcano

Kilauea Volcano is the youngest of five subaerial volcanoes on the island of Hawaii. The south flank of Kilauea Volcano (the area south of Kilauea's east and southwest rift zones) is the most actively deforming area in Hawaii, with strain rates a factor of 10 greater than the San Andreas fault and has experienced earthquakes with magnitudes greater than 7.0. It is thought by many to be the most likely site of a future major tsunami generating earthquake/landslide [*Lipmann et al.*, 1985]. It is also one of the

[1]Department of Aerospace Engineering Sciences, University of Colorado, Boulder, Colorado, USA.
[2]Department of Geophysics, Stanford University, Stanford, California, USA.
[3]U.S. Geological Survey, Cascades Volcano Observatory, Vancouver, Washington, USA.
[4]U.S. Geological Survey, Hawaiian Volcano Observatory, Hawaii Volcanoes National Parks, Hawaii, USA.
[5]Department of Earth Sciences, University of Southern California, Los Angeles, California, USA.

Paper number 2001JB000305.
0148-0227/01/2001JB000305$09.00

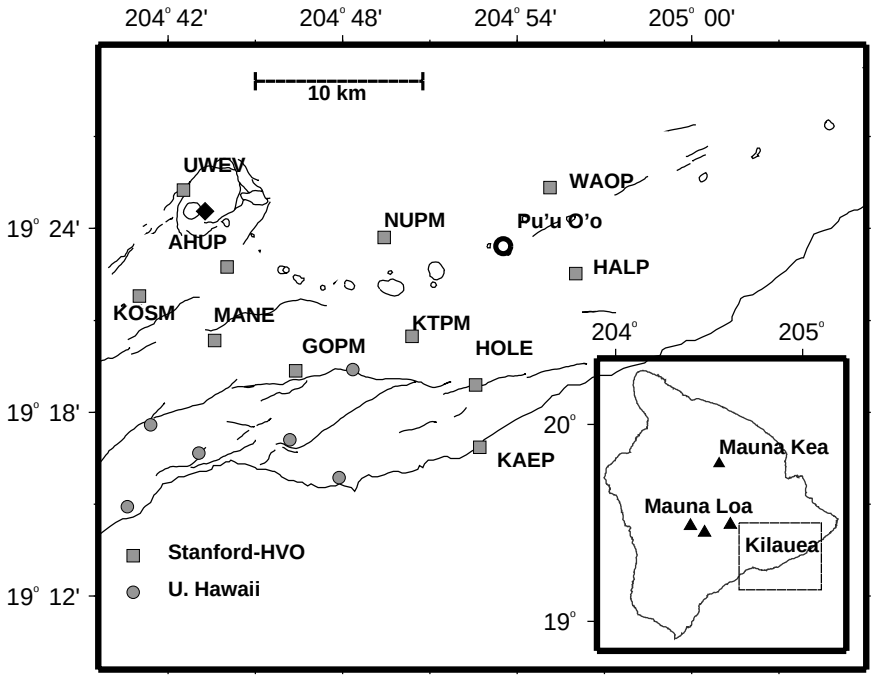

Figure 1. The HVO-Stanford Kilauea GPS network. All sites except HALP and WAOP were operating during this study. Also shown are other GPS sites operated by HVO (on Mauna Loa), the University of Hawaii, and JPL (on Mauna Kea). The Mogi source location used in the paper is shown as a diamond [*Owen*, 1998]. The location of Pu'u 'O'o is marked with an open circle.

most active volcanoes in the world. Kilauea's current eruption from Pu'u 'O'o or Kupaianaha vents in its east rift zone (Figure 1) has been almost continuously active since 1983 at an average rate of $\sim$0.1 km^3/yr.

Geodesy has long been used to monitor deformation of Kilauea Volcano, with the first triangulation survey begun in 1896. Most of these geodetic measurements, e.g., leveling and electronic distance measurements (EDM), require a significant level of human resources in the field, rendering these techniques ill-suited for hazard mitigation. GPS has been used to monitor deformation at Kilauea Volcano since 1987. Originally, GPS measurements at Kilauea were conducted in much the same manner as leveling and EDM, with annual or biannual campaigns. *Dvorak et al.* [1994] present results from the earliest surveys. Also using survey results, *Owen et al.* [1995] found that sites on the south flank of Kilauea moved seaward at rates of up to 10 cm/yr. Of course, there was no information on whether deformation rates varied at periods of less than a year.

Kilauea Volcano, with both long-term deformation and an active eruption history, requires more frequent observations. With this in mind, two continuously operating GPS sites were jointly installed by HVO and Stanford University in 1995. In subsequent years, more sites were installed. Currently, there are 12 GPS installations on Kilauea; 3 of these sites are "semipermanent" installations and can be moved. HVO also operates three GPS receivers on Mauna Loa, and NASA operates a site on nearby Mauna Kea. The University of Hawaii installed a six-station network on the southwest flank of Kilauea and operates it with the cooperation of HVO (see Figure 1), bringing the total to 22.

The performance of the continuous GPS network at Kilauea has been discussed elsewhere [*Owen*, 1998; *Owen et al.*, 2000a]. Generally, it has measured time-varying deformation rates at scales of hours to weeks. This was especially clear after the January 1997 East Rift Zone intrusion/fissure eruption, which produced more than 30 cm of displacement in less than a day at some sites. The goal of this project is to investigate GPS analysis strategies so that volcanic deformation on timescales of hours to days can be resolved in near real time.

3. GPS Analysis

GPS data analysis requires the availability of accurate orbit information, reasonable tracking geometry, proper models of propagation effects, and well-determined carrier phase biases. In this study the data were analyzed with the GIPSY software, which has the appropriate models and parameter estimation software [*Lichten and Border*, 1987].

A 140-day time period from 1998 was chosen to assess analysis strategies. While this time period is not long enough to study seasonal errors, the primary interest is the subdaily to weekly error spectrum. The start of the time series was chosen to coincide with the installation of a borehole tiltmeter at Uwekahuna, which is collocated with the GPS site Uwekahuna (UWEV) (Figure 1). The end of the time series coincided with firmware and hardware changes that were made to many of the receivers in the network.

The location of the eight HVO-Stanford sites are shown in Figure 1. GPS data were collected every 30 s, but the data were later decimated to 5-min intervals to reduce the computational burden and because of the strong temporal correlation of some error sources at high frequencies. This clearly limits how often receiver coordinates can be estimated but is appropriate for temporal scales of hours to days.

The raw 30-s data have been retained in the data archive and are available from UNAVCO (http://www.unavco.ucar.edu). The GIPSY software does not explicitly difference the GPS observables and satellite and receiver clocks are estimated at each data epoch. The clocks are determined relative to a reference clock; the receiver at Mauna Kea was chosen as the reference clock because it had the most stable oscillator in the network. The troposphere delay at zenith is estimated as a random walk process [*Lichten and Border*, 1987]. The tropospheric delay between each receiver and satellite

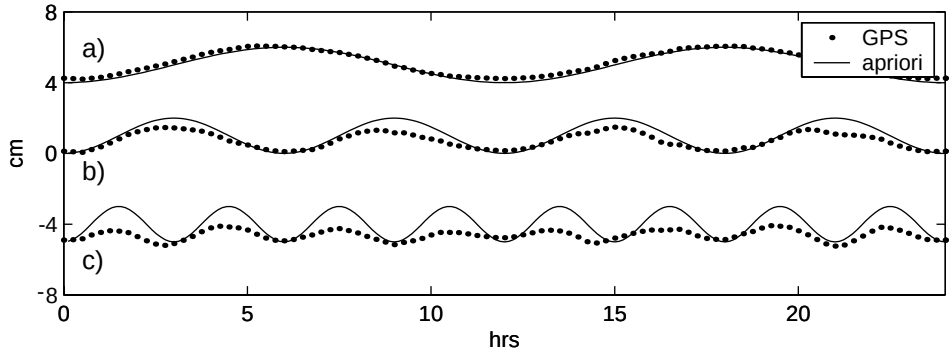

Figure 2. Solutions for the Uwekahuna-Ahua (UWEV-AHUP) baseline. In each case a sinusoid of amplitude of 1 cm was introduced into the data. The periods of the sinusoids are (a) 12 hours, (b) 6 hours, and (c) 3 hours.

is then calibrated via the estimated zenith delay and the Lanyi mapping function [*Lanyi et al.*, 1984]. Ionospheric effects are minimized by combining the dual-frequency data. Data below an elevation angle of 15° were not used to minimize errors due to multipath. Each solution was carefully checked for data outliers in the phase postfit residuals. All phase outliers that were larger than 5 cm were removed. For a fuller discussion of GIPSY analysis strategies, see, for example, *Larson et al.* [1997].

Precise satellite orbits produced by the International GPS Service (IGS) were used, with a range accuracy of 3–5 cm [*Beutler et al.*, 1994; *Kouba and Mireault*, 1996]. This is more than sufficient for a network of the spatial dimensions of Kilauea Volcano. Ultimately, predicted orbit products will be implemented into the network analysis (paper 2). Preliminary tests suggest that for the Kilauea network, predicted IGS orbits are of sufficient quality for subcentimeter differential positioning [*Gendt et al.*, 2000]. To reach this conclusion, baseline estimates were computed using both predicted and precise orbits; the difference between these two solutions was also computed. In general, the two baseline solutions agree well, with ~2 estimates during this period disagreeing by more than 10 mm.

Inaccurate baseline estimates due to orbit error will be strongly related to the quality of predicted orbits produced by the IGS during the period of our study. At a minimum, any user of predicted orbits needs to be aware that accuracy information is distributed in the IGS orbit products. Most users of IGS orbit products assume that all GPS orbits are equally well determined. This assumption is reasonable when the difference between orbits is at the level of 3–5 cm in range. Some predicted satellite orbits with accuracy levels of 2 m are present in the predicted orbit products, and if these satellites are not removed from the GPS analysis, one will see apparent ground motion. This has also been noted in GPS studies of the troposphere [*Kruse et al.*, 1999] and atomic clocks [*Larson et al.*, 2000]. It is still possible that baseline estimates computed using either predicted and precise orbit solutions will incorrectly estimate ground displacement.

Station positions were estimated every 15 min using GIPSY's Kalman filter. Higher estimation rates are possible with GIPSY, but this rate is consistent with crustal deformation rates observed by the borehole instruments on Kilauea and is sufficient to fulfill the scientific and hazards mitigation goals of this project.

All time-varying parameters in GIPSY are modeled as a first-order Gauss–Markov process [*Lichten and Border*, 1987]. The time-varying parameters are updated at the end of each time interval, or batch. GIPSY allows time-varying processes to be modeled as a "white noise" process, with no temporal correlation, a random walk process with infinite correlation, or with more general Gauss–Markov processes with intermediate correlation lengths, sometimes referred to as "colored noise" processes. Solutions were compared using different correlation lengths; the colored noise models were no more precise or accurate than a random walk model. For this reason, the focus in this paper will be a random walk model, which is well known in the geodetic literature, for example, *Herring et al.* [1990].

For a random walk the position of the GPS receiver, x, is defined:

$$x_{k+1} = x_k + w_k, \tag{1}$$

where w is random noise and the indices $k + 1$ and k refer to increments in time. The noise covariance q_k is

$$q_k = q(t_{k+1} - t_k) = q\Delta t \tag{2}$$

q then is the variance per unit time and generates the random walk [*The Analytic Sciences Corporation Technical Staff* , 1974].

Given the proper q, a random walk parameterization should be appropriate for slowly varying deformation that occurs over hours to days. It would not necessarily be appropriate for every type of deformation signal, such as shown in Figure 2. In this example a sinusoidal deformation signal was introduced into GPS data from the Kilauea network. In each case the amplitude of the sinusoid is 1 cm, and the time period is 24 hours. While the filter can track the long-period sinusoid (12 hours), it becomes increasingly less accurate at shorter periods (6 and 3 hours). Kalman filter constraints are also chosen to reduce noise in the position estimates, but a q value that is too small will reduce the amplitude of a real position signal if the deformation occurs very quickly, e.g., 10-cm deformation over 30 min rather than over 3 hours. These issues will be addressed in greater detail in section 5.

In the GIPSY software, $\sqrt{q}$ is an input and is called σ_{rw} in the GIPSY documentation [*Lichten and Border*, 1987]. The units of this parameter are km/$\sqrt{\text{s}}$. This nomenclature was also used by *Elosegui et al.* [1996]. To make it easier to understand, the units of this parameter have been converted to cm/$\sqrt{\text{h}}$ and will be referred to as σ_{Δ}.

4. Subdaily GPS Position Estimates

Although permanently installed GPS receivers generally operate continuously, the majority of papers describing GPS data analysis and geophysical applications continue to estimate a single station position over a 24-hour period [*Argus and Heflin*, 1995; *Bock et al.*, 1997; *Larson et al.*, 1997; *Bennett et al.*, 1999; *Dixon et al.*, 2000]. This is appropriate when deformation rates are small and vary slowly over periods of years. Volcano monitoring is one geophysical application where subdaily position estimates are necessary.

There has been limited modeling of subdaily estimates using GPS in the geophysical literature, notably *Genrich and Bock* [1992] and *Elosegui et al.* [1996]. In both papers the authors analyzed approximately a week of GPS data. In the work of *Genrich and*

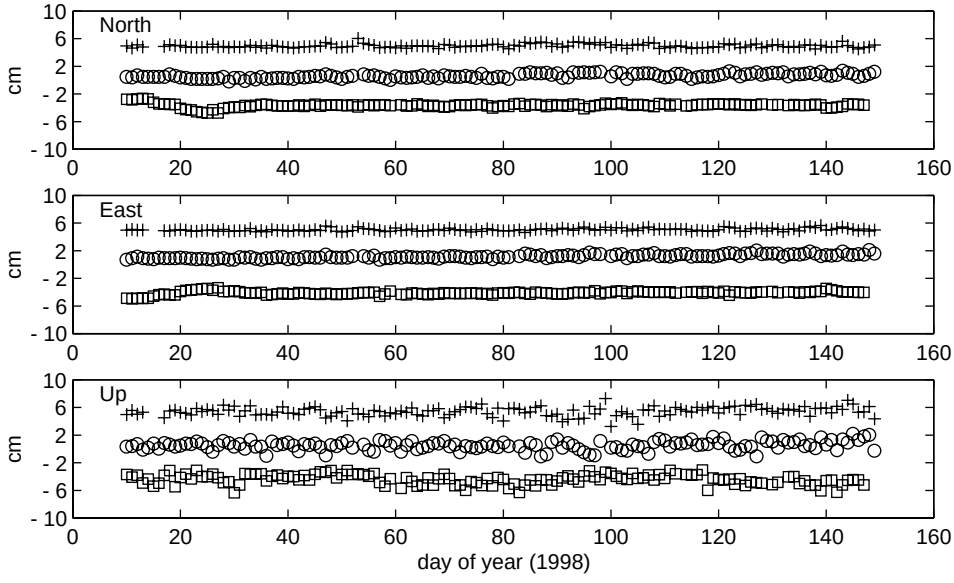

Figure 3. Twenty-four hour static solutions for baselines between Kalapana-Goat (KTPM-GOPM) (plus), Mauka Kipuka Nen-Nuio (MANE-NUPM) (circle), and UWEV-AHUP (square). The UWEV-AHUP baseline shows the effects of the January 15 summit inflation, which lasted for many weeks. For clarity, standard deviations are not shown for individual estimates but are generally 2, 2, and 6 mm for the east, north, and vertical components. An arbitrary constant has been removed from each time series. The location of each site is shown in Figure 1.

Bock [1992] their interest was in measuring static baselines over a short period of time, e.g., 30 min. Measurements were made at geodetic monuments where the assumption of zero motion is appropriate. White noise station solutions were computed at a rate of 1 Hz, and results were compared with solutions computed assuming no motion over 24 hours. *Genrich and Bock* [1992] also discussed the impact of the constellation on their solutions, concluding that good geometry (and observations from six or more satellites) is essential for precise 1-Hz position estimates.

Elosegui et al. [1996] presented analysis of GPS data for a different kind of experiment. They built an apparatus that moved a GPS antenna very slowly, 1 mm/h, and attempted to extract this velocity from GPS data collected for 24 hours. Unlike *Genrich and Bock* [1992], they used a random walk model for the station coordinates. It was demonstrated that the horizontal velocity could be accurately extracted with proper choice of σ_Δ.

Recent work by *Bock et al.* [2000] used white noise estimation of station positions. To remove the effects of multipath and other noise, a 3-day sidereal time-varying average of station positions is formed and subtracted, for example, from the station position estimates of the fourth day. This technique is computationally intensive and assumes that no deformation takes place on the three previous days.

The volcano monitoring system discussed here must be capable of measuring small deformation rates, $\sim$5–20 mm/h, but without the constraint that deformation rates will be linear. A further difficulty is calibrating the analysis technique. On Kilauea it cannot be assumed that the ground motion is zero [*Genrich and Bock*, 1992], and the true ground motion is not known, as in the work of *Elosegui et al.* [1996]. Instead, independent geodetic measurements from a borehole tiltmeter will be used to assess precision and accuracy, where available.

5. Results

5.1. Long-Term Motion

The long-term temporal characteristics of the data set are shown in Figure 3. Each symbol represents the daily baseline estimate, in north, east, and vertical components. This is the traditional GPS analysis strategy in which the station is assumed to be stationary for 24 hours. Three baselines are shown in Figure 3: Uwekahuna-Ahua (UWEV-AHUP) (5.3 km), Kalapana-Goat (KTPM-GOPM) (6.9 km), and Mauka Kipuka Nen-Nuio (MANE-NUPM) (11.5 km). (Additional baseline estimates for the Kilauea network are given by *Owen* [1998] and *Owen et al.* [2000a]). Defining precision as the weighted root-mean-square (RMS) about the best fit straight line yields 2.6, 1.9, and 6.3 mm for the north, east, and vertical components of the KTPM-GOPM baseline. If ambiguities had not been resolved, the north precision was unchanged, but the east and vertical precisions were degraded to 2.7 and 7.0 mm, respectively. The statistics for the MANE-NUPM baseline are similar, 1.7, 2.6, and 6.3 mm, for east, north, and vertical. It is not expected that the subdaily position will be better than the precision for 24-hour estimates. The UWEV-AHUP baseline shows evidence of nonlinear motion early in the time series that will be discussed later.

5.2. Spectral Analysis

A value of σ_Δ needs to be chosen that is appropriate for the temporal scales of deformation found in the data. At one end of the spectrum is a white noise estimation strategy, where almost no constraint is imposed on the coordinate estimates. A white noise estimation scheme will be comparable to a σ_Δ which is extremely large, e.g., 10^5 cm/$\sqrt{\text{h}}$. While significant deformation will still be observed with such an estimation strategy, smaller events will be obscured by system noise. If a value of σ_Δ is chosen which is too small, changes in the subdaily position estimates will be biased toward zero.

Figure 4 shows white noise baseline estimates for the KTPM-NUPM baseline. In other words, station positions were estimated every 15 min, and each position estimate is uncorrelated. This baseline was chosen because it is characteristic of the errors seen in other baselines and because there were no significant data outages at either KTPM or NUPM during this period. The length of the time series is 42.7 days or 4096 individual estimates. During this time period, there appeared to be no significant deformation of the baseline, which is consistent with its location far from the caldera. GIPSY requires an a priori station position uncertainty; 1 km was

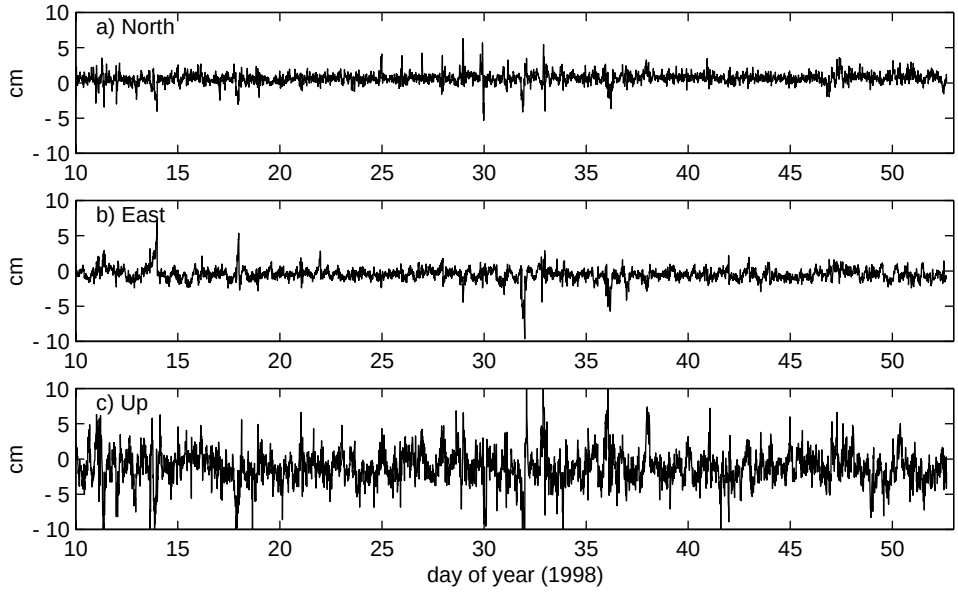

Figure 4. Fifteen-minute white noise baseline estimates for KTPM-NUPM (see Figure 1). The baseline is 5 km long; each estimate is independent.

used. As previously discussed by *Elosegui et al.* [1996] and others, white noise estimates are much more prone to solution outliers that are often caused by weak satellite geometry. The large outliers in Figure 4 are generally due to data loss, either because the receiver tracked poorly or because the automated data editor deleted too much data. A loosely constrained random walk solution, σ_Δ = 3 cm/$\sqrt{\text{h}}$, removes the large outliers near days 14 and 32 and produces a smoother solution (Figure 5). With the exception of outliers, the horizontal components in Figures 4 and 5 behave very similarly at periods less than 24 hours. In contrast, vertical component precision is dramatically improved by imposing a loose random walk constraint.

A variety of σ_Δ values were tested. The noise characteristics of these different time series can be better evaluated in the frequency domain. In Figure 6 the power spectral density for several random walk solutions is shown. Power spectral densities were computed using window lengths of 512 estimates; the data were overlapped by 256 estimates, windowed with a Hanning taper, and averaged, as by *King et al.* [1995]. There is little difference between the north and east component power spectral densities. At all periods the most tightly constrained solution, σ_Δ = 0.06 cm/$\sqrt{\text{h}}$, has lower power. The σ_Δ = 0.45−3.0 cm/$\sqrt{\text{h}}$ solutions are nearly identical at periods greater than 6 hours, at which point they diverge.

5.3. Ambiguity Resolution

There has been little published in the geophysical literature to describe the impact of ambiguity resolution on subdaily position estimates, although the impact on daily averages has been long

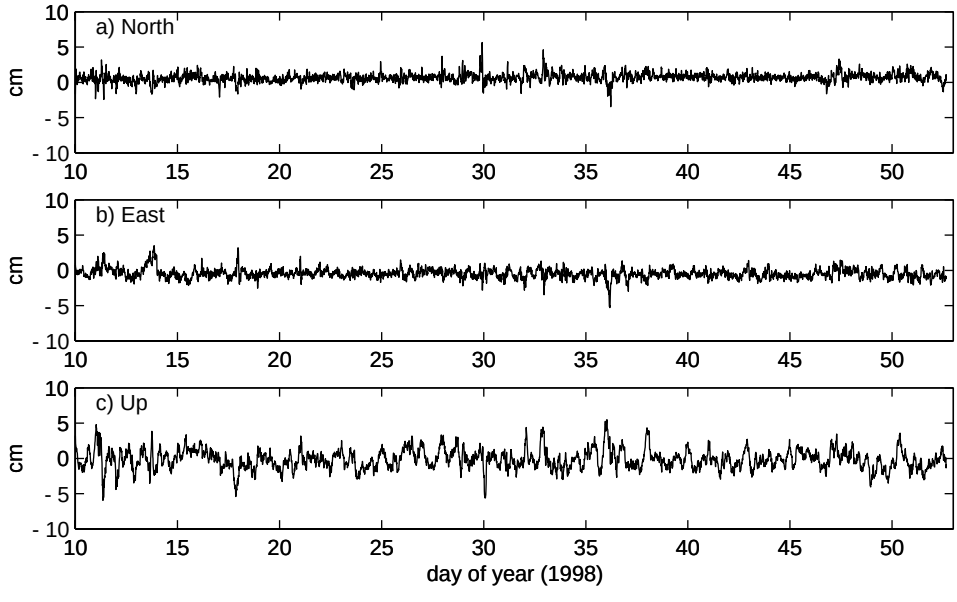

Figure 5. Fifteen-minute baseline estimates for KTPM-NUPM. A random walk constraint of σ_Δ = 3 cm/$\sqrt{\text{h}}$ was used.

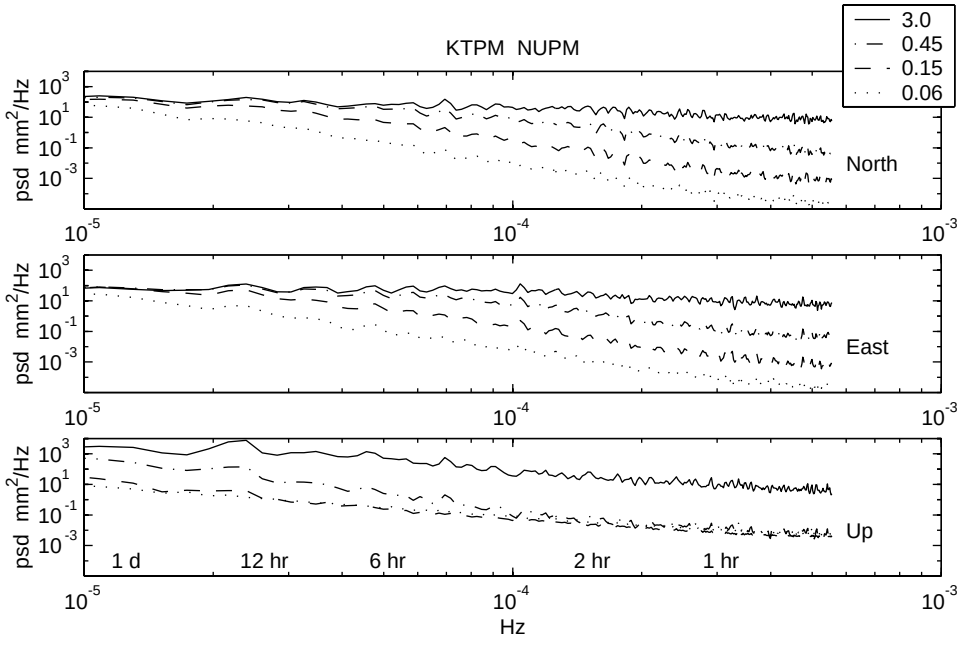

Figure 6. Power spectral density for random walk KTPM-NUPM estimates. The legend defines σ_Δ with units of cm/$\sqrt{\text{h}}$.

established [*Blewitt*, 1989; *Dong and Bock*, 1989]. Ambiguity resolution is of concern for this project because of near real-time constraints: ambiguity resolution increases CPU time used by GIPSY by almost 100%. Although currently there is ample time to compute subdaily position estimates on an hourly basis, eventually, the receiver download frequency may be increased, and whether ambiguity resolution is needed to achieve the goals of this project is still an open question.

The impact of ambiguity resolution can be easily described in the spectral domain. In Figure 7, solutions for σ_Δ = 3 cm/$\sqrt{\text{h}}$ are compared for the KTPM-NUPM baseline; the only difference between the solutions is ambiguity resolution. It is easily seen that ambiguity resolution has less impact at periods shorter than 4 hours. At longer periods the influence is component specific, with little impact on the north or vertical components. The east component shows significant improvement for periods between 6 hours and 1 day. Because crustal deformation on volcanoes is significant at these periods, ambiguity resolution will be required.

5.4. Choosing a Random Walk Constraint

Spectral analysis cannot find the optimal value of σ_Δ because suppressing high-frequency noise by using smaller values of σ_Δ will ultimately result in no change in station position at all. To choose the appropriate σ_Δ, it is necessary to compare the GPS estimates with an independent measurement system, preferably one with greater precision and accuracy. The borehole tiltmeter at

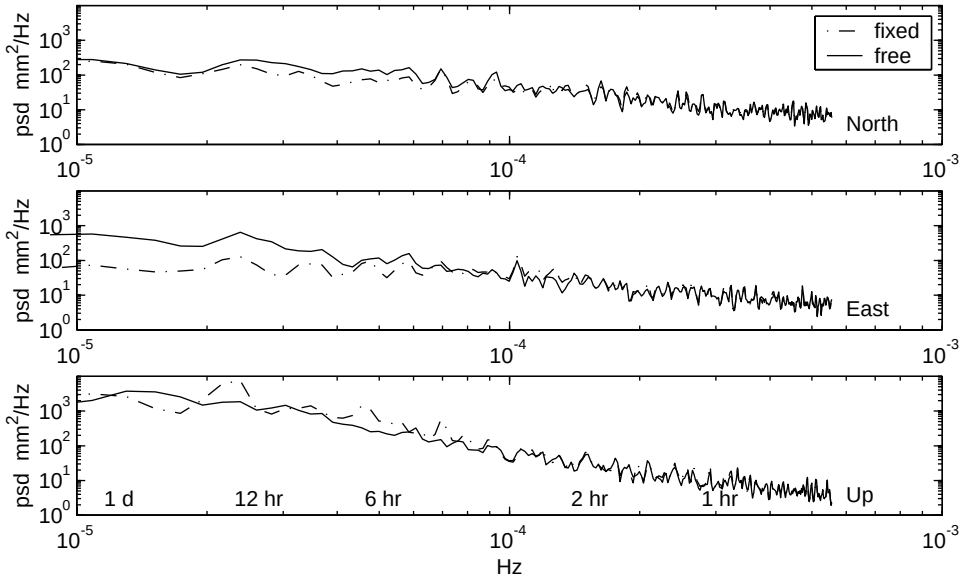

Figure 7. Power spectral density for random walk solutions, σ_Δ = 3 cm/$\sqrt{\text{h}}$, for carrier phase biases fixed and carrier phase biases not fixed. Note significant improvement at low frequencies for the east component.

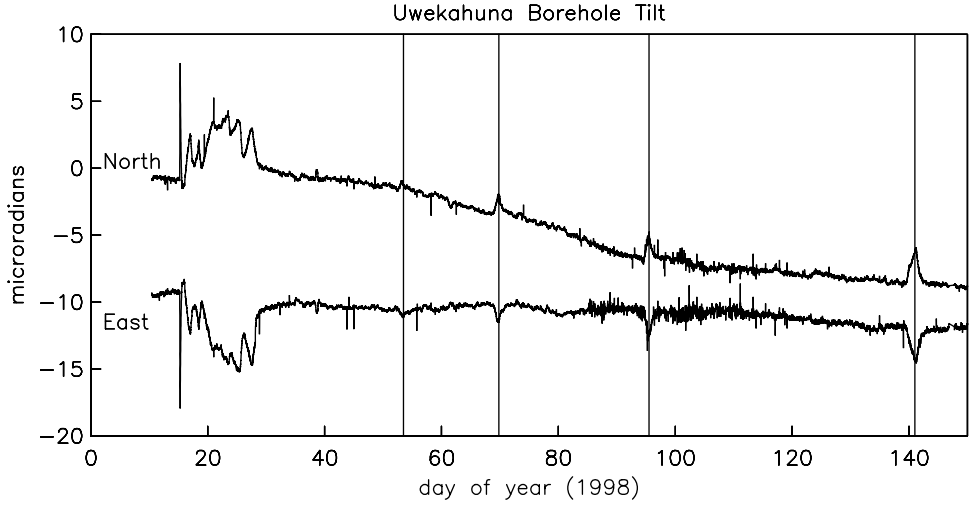

Figure 8. East and north component borehole tilt from the Uwekahuna site. Note the long-term drift in the north tilt component. Tilt noise is larger between days 85 and 110 due to electronic interference from newly installed equipment. Smaller summit inflation events are shown by vertical lines.

Uwekahuna, at 7-m depth, is nearly an order of magnitude more precise than GPS at short periods. The deeper installation makes it less susceptible to ground noise (diurnal and annual temperature cycles) than surface tiltmeters. The tiltmeter data were sampled every 10 min. Over the 5-month period of this study, there were several clearly observed events in the tilt data (Figure 8). These summit inflation events correlate with observations of lava flow rates at Pu'u 'O'o. The spikes in the tiltmeter data result from data transmission errors. (Beginning in 1999, the telemetry system used for the tiltmeter data was upgraded; this has effectively eliminated data transmission errors that were apparent during the period of this study.) The largest tilt event that occurred during this study is used to choose a proper σ_Δ value.

On January 15, 1998, the summit of Kilauea began to inflate rapidly. Within 3 hours, more than 12 μrad had been recorded on the Uwekahuna tiltmeter, followed by 5 hours of deflation to within 0.5 μrad of its preevent tilt value. There continued to be variations at the level of 2–4 μrad/d over the next 2 weeks. The initial inflation was accompanied by numerous small earthquakes, which were felt in the summit area. Pu'u 'O'o responded to the summit inflation by sending several lava flows onto the surface from vents on the south side of the edifice. Inflation at the summit of Kilauea should be observable in the UWEV-AHUP baseline. The location of the Mogi inflation-deflation source associated with recent eruptive/intrusive events is shown in Figure 1 [*Mogi*, 1958; *Owen et al.*, 2000b]. This model predicts radial motion about the source, and thus UWEV motion (N45°W with respect to the Mogi source) should be approximately equal in magnitude for the east and north components but opposite in sign. AHUP is located twice as far from the summit as UWEV (S21°E), so the deformation signal is expected to be both smaller at this site and larger in the southward direction than the eastward direction. More complex

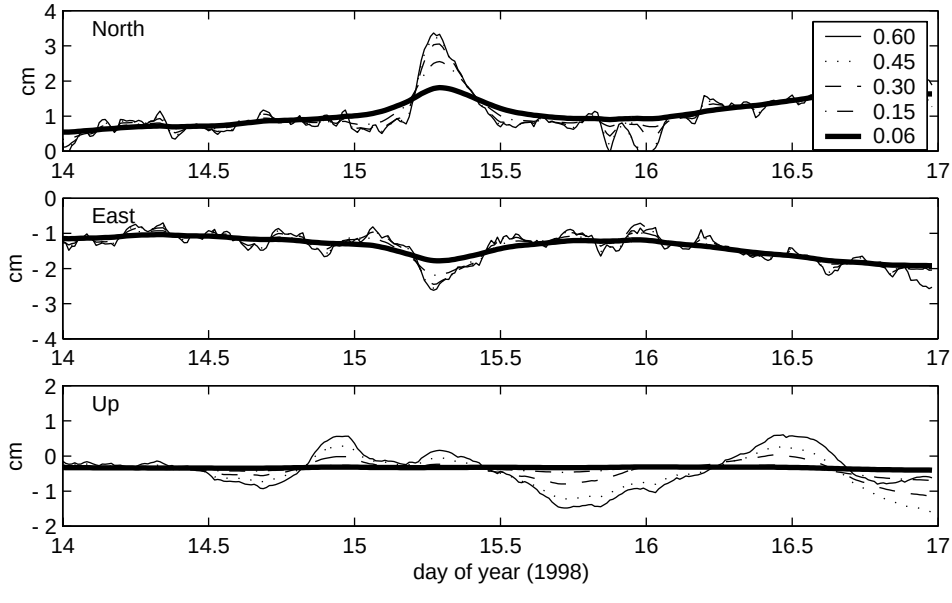

Figure 9. Fifteen-minute GPS position estimates for the UWEV-AHUP baseline on January 15, 1998, for σ_Δ ranging from 0.06 to 0.60 cm/$\sqrt{\text{h}}$.

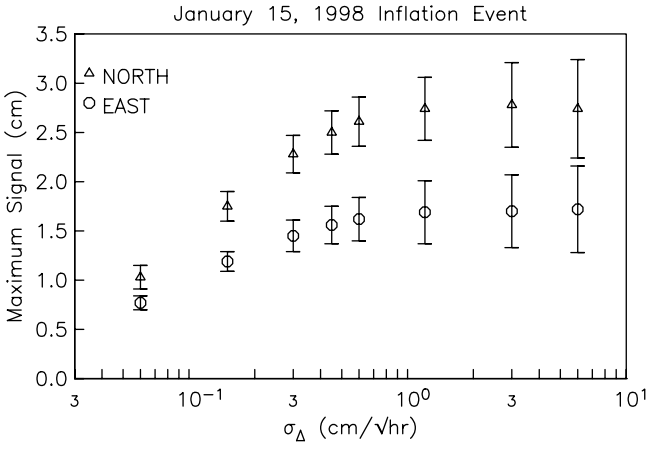

Figure 10. Maximum signal between UWEV and AHUP on January 15, 1998, as a function of σ_Δ. The error bars are one standard deviation, calculated as the RMS over 4 hours.

source models will not predict perfectly radial motion at UWEV and AHUP and that there are also uncertainties associated with the Mogi source location.

Figure 9 shows a suite of random walk solutions for the UWEV-AHUP baseline, with σ_Δ ranging from 0.06 to 0.60 cm/$\sqrt{\text{h}}$. The true signal is clearly dampened for σ_Δ values between 0.06 and 0.30 cm/$\sqrt{\text{h}}$, with convergence between 0.45 and 0.60 cm/$\sqrt{\text{h}}$. Note how the high-frequency noise in the baseline estimates increases as σ_Δ becomes larger. For completeness, the vertical estimates are shown for all cases, although deformation associated with inflation/deflation of the caldera is not resolvable.

Figure 10 summarizes the size of the inflation signal as a function of σ_Δ and makes the tradeoff between high frequency noise and signal suppression more clear. The error bars shown in Figure 10 were determined from the RMS of the estimates for 4 hours prior to the event. If error bars are computed using different time periods (between 1 and 6 hours), the resulting trade-off shows that 0.45 cm/$\sqrt{\text{h}}$ allows an unbiased estimate of the event and significantly suppresses high-frequency noise. A trade-off for vertical estimates is not shown as the estimates do not show a clear correlation with the event. For a large enough signal, such as the January 30, 1997, fissure eruption, the vertical component will provide important constraints on the deformation process.

Are the subdaily position estimates shown in Figure 9 consistent with the tilt data? In order to compare the two data types, the Mogi source location of *Owen et al.* [2000b] was used, which itself was derived from geodetic data collected during the January 30, 1997, event; its location with respect to the GPS instruments is shown in Figure 1. While borehole tilt precision is very good (RMS of 0.1 μrad over 1 day), the orientation of the tiltmeters is not currently known to better than 5°. In order to compare the tilt and GPS data a proportionality constant must be determined. An impulse function was created that basically mimics the tilt data on January 15; this impulse and the Mogi model were used to calculate surface tilts at Uwekahuna. The tilt data were then rotated until they agreed with the model predictions. In other words, the east and north tilt data agree perfectly (within 0.2 μrad) with the Mogi model. This rotation was less than the expected uncertainty in the tilt orientation. The same impulse and Mogi model were then used to calculate surface displacements at UWEV and AHUP. In Figure 11 the Mogi model predictions and GPS position estimates are compared. The temporal variations between the model predictions and the GPS estimates agree very well. The model slightly underpredicts the amplitude of the north component deformation between UWEV and AHUP but is in good agreement in the east component. Clearly, no vertical deformation signal has been observed. Given the unphysical approximations in the Mogi model, uncertainties in the Mogi source location, elastic heterogeneity, and the tiltmeter orientation ambiguity, the agreement between the GPS position estimates and the Mogi model is very good.

5.5. Solution Quality

Figure 12 summarizes the UWEV-AHUP time series for the 140-day period using a σ_Δ of 0.45 cm/$\sqrt{\text{h}}$. For comparison, the tilt in the west direction is also shown (both tilt records were shown in

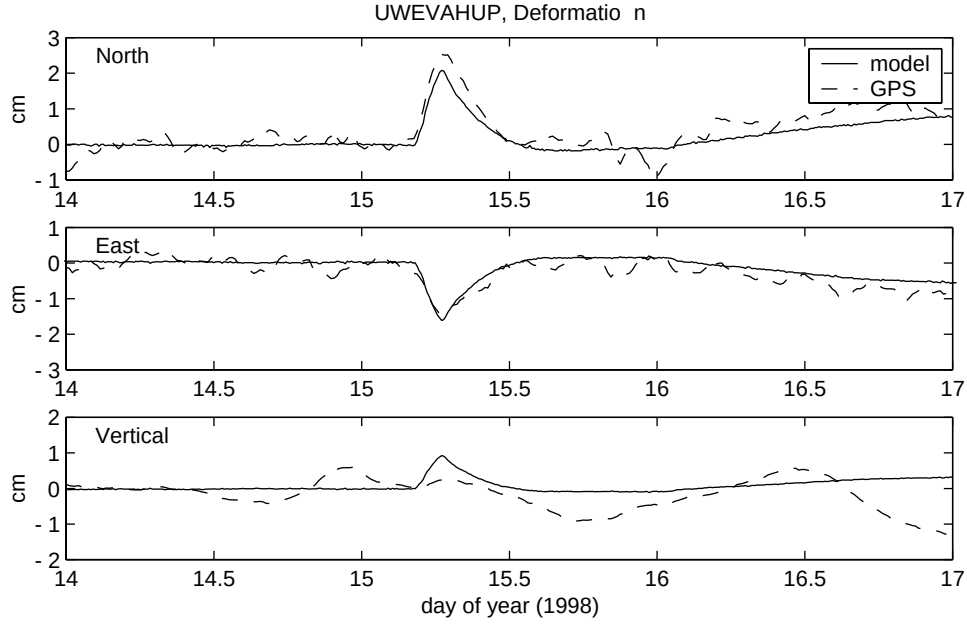

Figure 11. GPS observations and Mogi model predictions for the January 15, 1998, summit inflation event. The time dependence of the Mogi model predictions is based on borehole tilt records. The GPS solutions were computed using a σ_Δ of 0.45 cm/$\sqrt{\text{h}}$. The Mogi source location is taken from *Owen et al.* [2000b].

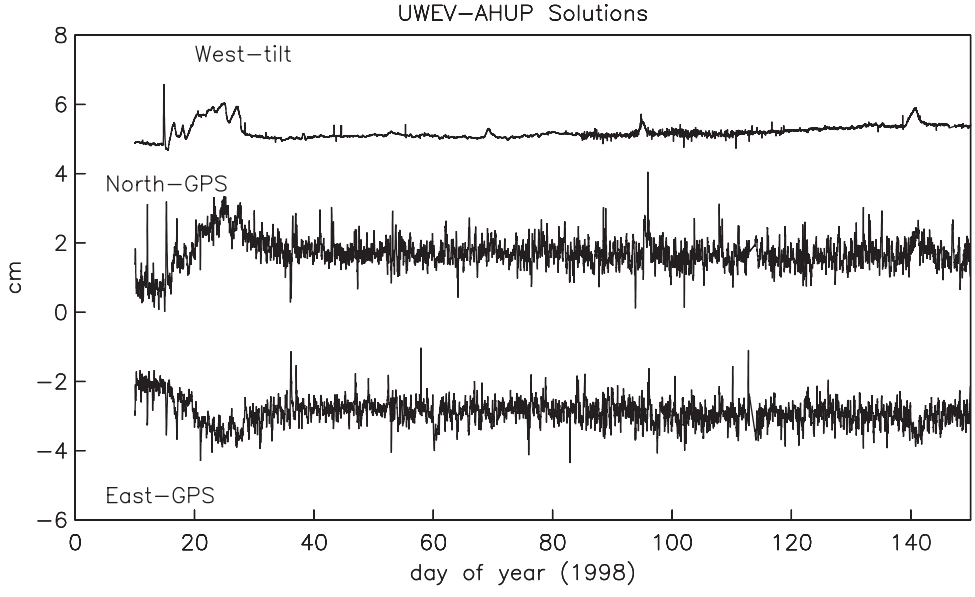

Figure 12. Horizontal baseline solutions for the UWEV-AHUP baseline for σ_Δ = 0.45 cm/$\sqrt{\text{h}}$. There are no AHUP data for day 60 and day 118. West component Uwekahuna tilt records are also shown, using a scale factor of 0.19 cm/μrad.

Figure 8). The tilt data have outliers on occasion (two are shown near day 45), but these outliers are generally only one point in the data stream, easily identified and removed. The nature of GPS baseline (or position) outliers is quite different, with outliers being highly correlated over periods of 1–4 hours. In Figure 12 it can be seen that the GPS time series shows good agreement with the tilt data during the January 15 inflation event and its aftermath. It also agrees with much smaller long-period inflation events at days 94 and 140. Nevertheless, there are several baseline estimates of the same magnitude (although not the same duration) as the January 15 event that were not observed by the borehole tiltmeter. If these GPS position estimates correlated with an increase in the estimate standard deviations, i.e., formal errors, this would not be of great concern, as it would be possible to minimize the significance of the position estimate in both the source model and hazards mitigation studies. The larger formal errors might indicate, for example, that several satellites were missing during that time interval.

The data analyzed for this study show that the GIPSY-derived formal errors do not indicate that a baseline determination is in error. To evaluate the quality of the estimates, more information is needed. The following questions were investigated:

1. Are the baseline estimate outliers specific to GIPSY analysis?
2. Do the signal-to-noise ratios data indicate anomalies?
3. Are the baseline estimates sensitive to changing the elevation angle cutoff?
4. Do the solution outliers correlate with changes in the zenith troposphere delay?

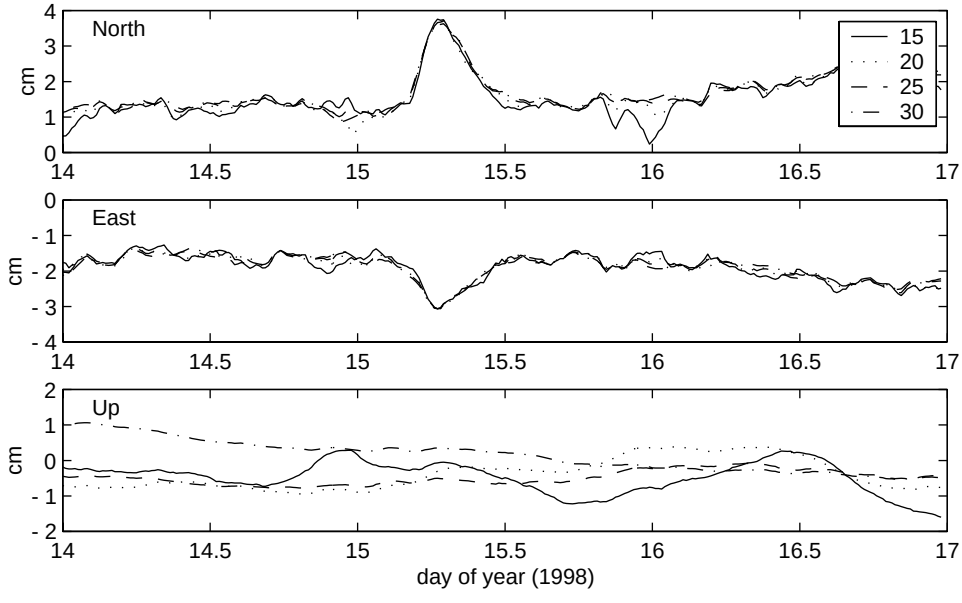

Figure 13. Baseline solutions for the UWEV-AHUP baseline, σ_Δ = 0.45 cm/$\sqrt{\text{h}}$, at elevation angle cutoffs between 15° and 30°.

Table 1. Outliers, UEV-AHUP[a]

Day of year	Elevation Cutoff					
	North			East		
	15	20	25	15	20	25
36.25	-	-	-	1.3	1.0	0.8
93.75	1.6	1.4	1.3	-	-	-
95.25	1.8	1.9	1.4	-	-	-
112.75	-	-	-	1.0	0.6	0.5
122.25	1.0	1.0	0.9	-	-	-
135.25	1.3	1.3	0.9	-	-	-

[a]Outlier size, in centimeters, with respect to the mean of the previous 12 hours of UWEV-AHUP baseline estimates.

From limited tests, significant GIPSY specific errors have not been found. Solutions were compared with both GAMIT [*Dong and Bock*, 1989] and commercial software, and the outliers were present in all software solutions. The signal-to-noise ratio data were also investigated to determine if multipath could explain the outliers in the solutions [*Axelrad et al.*, 1996]. Nothing was found that would indicate an anomaly at these times.

The presence of unmodeled elevation angle dependent errors in the GPS observations can be demonstrated by changing the elevation angle cutoff and comparing the different solutions. Multipath is one example of an elevation angle dependent error source. Multipath is not modeled in GIPSY (nor in any other geodetic software package), so if there is a significant multipath problem at a site, this can corrupt the baseline estimates, particularly the height [*Elosegui et al.*, 1995]. Multipath can also produce errors in daily static GPS solutions, but as long as the multipath environment stays the same, the error will be a constant bias, which is not a concern for most crustal deformation studies. The troposphere delay has a direct dependence on elevation angle, so if the delay is not properly modeled, this can easily impact other estimated parameters, including position. This is not a problem unique to GPS. Least squares analysis will always attempt to distribute misfit among other parameters. If the only contribution to the GPS data is due to station position changes, there should be no simultaneous changes in the other estimated parameters, such as the tropospheric delay (unless of course a station moved at the same time the weather dramatically changed).

Baseline solutions were computed for the largest deformation signal in this study, the January 15 inflation event; no significant variation was found in the horizontal signal size between elevation angle cutoffs of 15° and 30° (Figure 13). The primary benefit of raising the cutoff is smoother solutions at higher frequencies. Continuing to raise the cutoff ultimately hurts both horizontal and vertical components because fewer satellites will be in view. While the vertical component becomes smoother as the cutoff is raised, the estimate clearly becomes biased at a cutoff of 30°, with a significant trend with respect to the "truth." No correlation was found between troposphere estimates and position estimates during the January 15 inflation event.

We next investigated times when the GPS estimates did not agree with the tiltmeter data. GPS estimate standard deviations did not explain the position changes. By examining the RMS agreement between the tilt and GPS solutions over a 12-hour period, we found six outlier solutions greater than 5 mm. For each of these cases we examined the solutions for elevation cutoffs of 15°, 20°, and 25° (Table 1). Figure 14 is representative of what we found. There is a strong correlation between the outlier and the troposphere estimate and the ground displacement was reduced by 25% by changing the elevation angle cutoff from 15° to 20°. This was not the case when ground displacement really occurred. As one would expect, we detected more "false" outliers using 15° cutoff solutions than with 20° cutoff solutions. This suggests that any triggering algorithm that is implemented on Kilauea will compute two baseline solutions: one using a standard elevation angle cutoff of 20° and another at 25°. While this might suggest that the necessary computations will be doubled, the GIPSY software has the flexibility to augment one solution (computed with a cutoff of 20°) by removing all the observations below 25° without additional filtering. The additional computing required is of the order of 10%. Furthermore, these computations will only be required when ground displacement is suspected.

5.6. Tracking Large Deformation Signals

Although the resolution of the January 15 inflation event is quite good, it could be argued that the 5-month time period used in this study is not representative of volcanic deformation signals, particularly large ones. The random walk constraints proposed for the Kilauea GPS Network, 0.45–0.60 cm/$\sqrt{\text{h}}$ have been extensively tested on the larger fissure eruption of January 30, 1997, which produced displacements as large as 20 cm in 8 hours. However, how would the filter respond to even larger events at shorter time periods? The tilt data from January 15 were used to simulate a much larger inflation event, with a maximum amplitude of 40 cm reached in less than 3 hours (Figure 15). The GPS results are

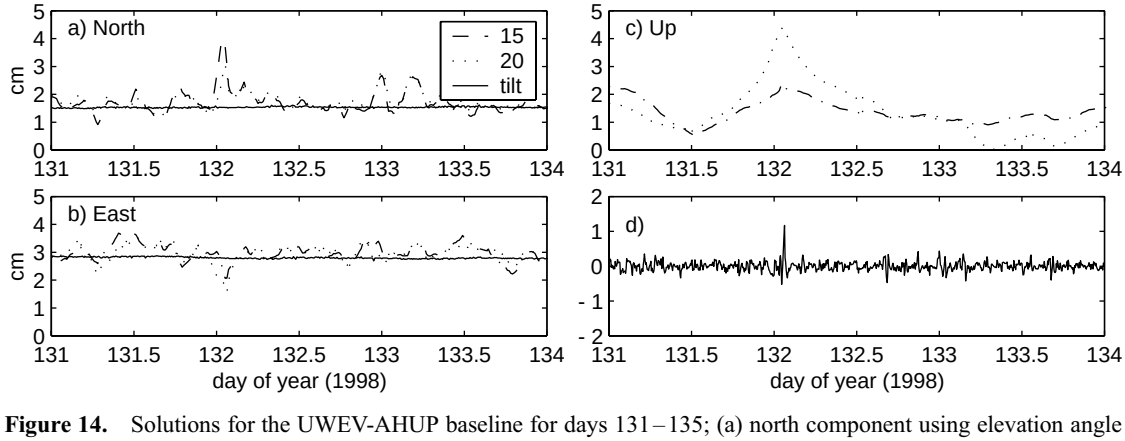

Figure 14. Solutions for the UWEV-AHUP baseline for days 131–135; (a) north component using elevation angle cutoffs of 15° and 20°; (b) east and vertical components; (c) first difference of zenith troposphere delay, i.e., $tr_2 - tr_1$, $tr_3 - tr_2$, where tr_i is the zenith troposphere delay at epoch i. The size of the peak in the north component at day 132 is decreased when the minimum elevation angle is raised to 20°. There are coincident peaks in the east and vertical components and in the troposphere difference.

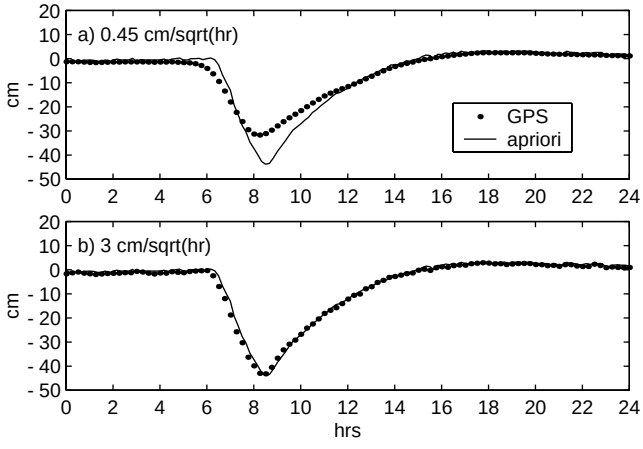

Figure 15. Solutions for the UWEV-AHUP baseline for 24 hours. In each case the January 14, 1998, tilt event was introduced into the data and amplified by a factor of 20. The GPS data were then analyzed using a σ_Δ of (a) 0.6 and (b) 3.0 cm/$\sqrt{\text{h}}$. The onset and amplitude of this large event in this case are better resolved using the looser σ constraint.

shown for σ_Δ values of 0.45 and 3 cm/$\sqrt{\text{h}}$. Clearly, for this case the smaller value is inadequate. It does a poor job of resolving the onset of the event and it suppresses the true amplitude by 20%. In cases where the near real-time GPS solutions as well as other data sets find that large-amplitude events are in progress, the GPS analysis software should automatically produce more loosely constrained solutions.

6. Discussion

Since the Uwekahuna tiltmeter unambiguously observed all inflation events during this 5-month period (Figure 8), without complicated data analysis, is there any value in producing high-frequency GPS solutions? We would argue that there is. The GPS instruments have been installed because they provide a stable three-dimensional positioning capability. They are currently operating at fixed sites but are flexible enough that a GPS system can be quickly installed at the first sign of unrest. This system can then easily be included in network analysis at no additional cost. Installation of a borehole tiltmeter is a significant cost and is not something that can be installed during a crisis situation.

Because tilt is the spatial derivative of the vertical displacement, broad-scale deformation might be missed or misinterpreted by a geodetic network that contained only tiltmeters, particularly if the scale of the deformation field is significantly larger than the scale of the tilt network. If the entire caldera were to uplift dramatically at say meters per day, the tilt signal might not be so dramatic since it senses only the derivative of the uplift at each tilt station. The errors in the two instruments are also quite different. While tilt is much more precise than GPS at short periods, it correlates strongly with environmental factors like heavy rainfall. Tiltmeters also appear to have significant drifts at periods of more than a few weeks. More work needs to be done comparing the two data types over long periods.

A combination of the two instruments seems to be the best geodetic volcano monitoring system. Obviously, a signal that shows up on both instruments is much more believable than a signal observed on either instrument individually. The tilt data are of great value at periods less than a day. GPS data can suppliment the tiltmeter at these periods for deformation signals greater than 5 mm, as well as providing important constraints on deformation where tiltmeters have not been installed. Combining the two data types will be important for near real time source inversion (paper 2).

7. Conclusions

By appropriate use of available telemetry systems, it is conceptually straightforward to upgrade a continuously operating GPS network into one where analysis is nearly continuous and real time. In regions where crustal deformation rates are either low or linear and there is no risk to humans or human infrastructure, there is little incentive to install such systems. In volcano monitoring both a near real-time data stream and the ability the estimate deformation at periods well below the typical analysis strategies are needed. In this study it is shown that a random walk parameterization of ground displacement is well-suited for characterizing baseline changes on a volcano. Although large displacements were not observed during the period of this study, smaller inflation events that had amplitudes as low as 1 cm, with periods from 6 hours to 2 days, were observed. In addition to formal errors, tools were developed to ensure solution quality by using elevation angle cutoff tests. In doing so a technique that relates to known limitations in the GPS models is being used. Information related to the reasonableness of the estimated surface deformation in terms of the known geologic structures of Kilauea Volcano has not been utilized. Nor does this paper address the critical issues of combining tilt and GPS data and robust triggering algorithms. These issues will be discussed in detail in paper 2.

Acknowledgments. K.L. would like to thank HVO and Stanford University for hosting her sabbatical. Funding for this sabbatical was provided by NSF's Professional Opportunities for Women in Research and Education (POWRE) program. The USGS-Stanford Kilauea GPS network has been supported by NSF and USGS NEHRP. The authors thank Tim Dixon, Al Linde, and Chuck Connor for very constructive reviews that significantly improved the paper.

References

Argus, D., and M. Heflin, Plate motion and crustal deformation estimated with geodetic data from the Global Positioning System, *Geophys. Res. Lett.*, *22*, 1973–1976, 1995.

Axelrad, P., C. J. Comp, and P. F. MacDoran, SNR based multipath error correction for GPS differential phase, *IEEE Trans. Aerosp. Electron. Syst.*, *32*(2), 650– 660, 1996.

Bennett, R. A., J. L. Davis, and B. P. Wernicke, Present-day pattern of Cordilleran deformation in the western United States, *Geology*, *27*(4), 371–374, 1999.

Beutler, G., I. I. Mueller, and R. E. Neilan, The International GPS Service for Geodynamics (IGS): Development and start of official service on January 1, 1994, *Bull. Geod.*, *68*(1), 39–70, 1994.

Blewitt, G., Carrier phase ambiguity resolution for the Global Positioning System applied to geodetic baselines up to 2000 km, *J. Geophys. Res.*, *94*, 10,187–10,203, 1989.

Bock, Y., et al., Southern California Permanent GPS Geodetic Array: Continuous measurements of regional crustal deformation between the 1992 Landers and 1994 Northridge earthquakes, *J. Geophys. Res.*, *102*, 18,013–18,033, 1997.

Bock, Y., R. M. Nikolaidis, P. J. de Jonge, and M. Bevis, Instantaneous geodetic positioning at medium distances with the Global Positioning System, *J. Geophys. Res.*, *105*, 28,223–28,253, 2000.

Dixon, T. H., A. Mao, M. Bursik, M. Heflin, J. Langbein, R. Stein, and F. Webb, Continuous monitoring of surface deformation at Long Valley Caldera, California, with GPS, *J. Geophys. Res.*, *102*, 12,017–12,034, 1997.

Dixon, T., M. Miller, F. Farina, H. Wang, and D. Johnson, Present-day motion of the Sierra Nevada block and some tectonic implications for the Basin and Range province, North American Cordillera, *Tectonics*, *19*, 1–4, 2000.

Dong, D., and Y. Bock, Global Positioning System network analysis with phase ambiguity resolution applied to crsutal deformation studies in California, *J. Geophys. Res.*, *94*, 3949–3966, 1989.

Dvorak, J., F. Klein, and D. Swanson, Relation of the south flank after the 7.2 magnitude Kalapana earthquake, Kilauea Volcano, Hawaii, *Bull. Seismol. Soc. Am.*, *84*, 133–141, 1994.

Elosegui, P., J. Davis, R. Jahldehag, J. Johansson, A. E. Niell, and I. Shapiro, Geodesy using the Global Positioning System: The effects of signal scattering on estimates of site position, *J. Geophys. Res.*, *100*, 9921–9934, 1995.

Elosegui, P., J. Davis, J. Johansson, and I. Shapiro, Detection of transient

motions with the Global Positioning System, *J. Geophys. Res.*, *101*, 11,249–11,261, 1996.

Gendt, G., P. Fang, and J. Zumberge, Moving IGS products towards real-time, in *Proceedings of the 1999 IGS Analysis Center Workshop*, pp. 391–403, IGS Cent. Bur., Pasadena, Calif., 2000.

Genrich, J., and Y. Bock, Rapid resolution of crustal motion at short ranges with the Global Positioning System, *J. Geophys. Res.*, *97*, 3261–3269, 1992.

Herring, T., J. Davis, and I. Shapiro, Geodesy by radio interferometry: The application of Kalman filtering to the analysis of very long baseline interferometry data, *J. Geophys. Res.*, *95*, 12,561–12,581, 1990.

King, N., J. Svarc, E. Fogleman, W. Gross, K. Clark, G. Hamilton, C. Stiffer, and J. Sutton, Continuous GPS observations across the Hayward fault, California, 1991–1994, *J. Geophys. Res.*, *100*, 20,271–20,283, 1995.

Kouba, J., and Y. Mireault, IGS Analysis Coordinator Report, in *IGS 1995 Annual Report*, edited by J. Zumberge et al., pp. 45– 77, IGS Cent. Bur., Jet Propul. Lab., Pasadena, Calif., 1996.

Kruse, L., B. Sierk, T. Springer, and M. Cocard, GPS meterology: Impact of predicted orbits on precipitable water estimates, *Geophys. Res. Lett.*, *26*, 2045–2048, 1999.

Lanyi, Tropospheric calibration in radio interferometry, in *Proceedings of the International Symposium on Space Techniques for Geodynamics*, edited by J. Somogyi and C. Reigber, pp. 184–195, IAG/COSPAR, Sopron, Hungary, 1984.

Larson, K. M., J. Freymueller, and S. Philipsen, Global plate velocities from the Global Positioning System, *J. Geophys. Res.*, *102*, 9961–9981, 1997.

Larson, K., J. Levine, L. Nelson, and T. Parker, Assessment of GPS carrier-phase stability for time-transfer applications, *IEEE Trans. Ultrason. Ferroelectr. Freq. Control*, *47*(2), 484– 494, 2000.

Lichten, S., and J. Border, Strategies for high-precision Global Positioning System orbit determination, *J. Geophys. Res.*, *92*, 12,751–12,762, 1987.

Lipmann, P. W., J. P. Lockwood, R. T. Okamura, D. A. Swanson, and K. M. Yamashita, Ground deformation associated with the 1975 magnitude-7.2 earthquake and resulting changes in activity of Kilauea Volcano, Hawaii, *U.S. Geol. Surv. Prof. Pap.*, *1276*, 45 pp., 1985.

Mattiloi, G. S., T. H. Dixon, F. Farina, E. S. Howell, P. E. Jansma, and A. L. Smith, GPS measurement of surface deformation around Soufriere Hills Volcano, Montserrat, from October 1995 to July 1996, *Geophys. Res. Lett.*, *25*, 3417–3420, 1998.

Miyazaki, S., and Y. Hatanaka, Crustal Deformation observed by GSI's new GPS array, *Eos Trans. AGU*, *78*(17), Spring Meet. Suppl., S104, 1997.

Mogi, K., Relations between the eruptions of various volcanoes and the deformations of the ground surfaces around them, *Bull. Earthquake Res. Inst. Univ. Tokyo*, *36*, 99–134, 1958.

Owen, S., P. Segall, J. Freymueller, A. Miklius, R. Denlinger, T. Arnadottir, M. Sako, and R. Burgmann, Rapid deformation of the South Flank of Kilauea Volcano, Hawaii, *Science*, *267*, 1328–1332, 1995.

Owen, S., GPS measurements and kinematic models of the surface deformation on Kilauea Volcano, Hawaii, Ph.D. dissertation, Stanford Univ., Stanford, Calif., 1998.

Owen, S., P. Segall, M. Lisowski, A. Miklius, R. Denlinger, and M. Sako, The rapid deformation of Kilauea volcano: GPS measurements between 1990 and 1996, *J. Geophys. Res.*, *105*, 18,983–18,998, 2000a.

Owen, S., P. Segall, M. Lisowski, M. Murray, M. Bevis, and J. Foster, The January 30, 1997 eruptive event on Kilauea Volcano, Hawaii, as monitored by continuous GPS, *Geophys. Res. Lett.*, *27*, 2757–2760, 2000b.

Stefansson, R., K. Agustsson, G. Gudmundsson, B. Thorbjarnard, and P. Einarsson, A successful prediction and warning of an eruption in the Hekla Volcano, Iceland, *Eos Trans. AGU*, *81*(19), Spring Meet. Suppl., S442, 2000.

The Analytic Sciences Corporation Technical Staff, *Applied Optimal Estimation*, edited by A. Gelb, MIT Press, Cambridge, Mass., 1974.

Zumberge, J., M. Heflin, D. Jefferson, M. Watkins, and F. Webb, Precise point positioning for the efficient and robust analysis of GPS data from large networks, *J. Geophys. Res.*, *102*, 5005–5018, 1997.

P. Cervelli and P. Segall, Department of Geophysics, Stanford University, Stanford, CA 94305, USA. (cervelli@pangea.stanford.edu; segall@pangea.stanford.edu)

K. M. Larson, Department of Aerospace Engineering Sciences, University of Colorado, Campus Box 429, Boulder, CO 80309-0429, USA. (kristine.larson@colorado.edu)

M. Lisowksi, Cascades Volcano Observatory, U.S. Geological Survey, 5400 MacArthur Blvd., Vancouver, WA 98661, USA. (mlisowski@usgs.gov)

A. Miklius, Hawaiian Volcano Observatory, U.S. Geological Survey, 51 Crater Rim Drive, Hawaii Volcanoes National Parks, HI 96718, USA. (asta@usgs.gov)

S. Owen, Department of Earth Sciences, University of Southern California, 3651 Trousdale Parkway, Los Angeles, CA 90089, USA. (owen@terra.usc.edu)

(Received June 12, 2000; revised December 13, 2000;
accepted April 12, 2001.)